

Model of multifragmentation, Equation of State and phase transition

C. B. Das¹, S. Das Gupta¹ and A. Z. Mekjian²

¹*Physics Department, McGill University, Montréal, Canada H3A 2T8*

²*Department of Physics and Astronomy, Rutgers University, Piscataway, New Jersey 08855*
(February 9, 2020)

We consider a soluble model of multifragmentation which is similar in spirit to many models which have been used to fit intermediate energy heavy ion collision data. We draw a p-V diagram for the model and compare with a p-V diagram obtained from a mean-field theory. Very large differences are found. We investigate the question of chemical instability in the multifragmentation model. Phase transitions in the model are discussed.

25.70.-z,25.75.Ld,25.10.Lx

I. INTRODUCTION

Statistical models of multifragmentation have long been used to explain data from heavy ion collisions. Such a model was first invoked for Bevalac results [1,2] and similar physical ideas but with many substantial variations were subsequently used for intermediate energy heavy ion collisions [3–5]. In this work we consider a model of multifragmentation, variations of which have found many applications in the literature [6–11,13]. Thermodynamic properties of a simpler version of this model have also been discussed [15–17]. The model we use here has two kinds of particles but no Coulomb interaction. Throughout the rest of this paper we will refer to this model as the thermodynamic model. Typically the number of particles in our model is 200 although we also use systems containing as many as 1000 particles. While we could have easily included a Coulomb interaction term, our objective here is different. The objective is to highlight some features which are present both in the thermodynamic model and in mean-field theories when mean field theories are applied to intermediate energy heavy ion physics. Typically mean-field theories use homogeneous infinite matter (hence no surface energy terms) and no Coulomb interaction. Finite systems with Coulomb and surface terms have also been included [14] in mean-field models but this makes discussions more complicated and we want to stay at the simplest level. As shown in [6] surface energy terms play an important role in a thermodynamic model and are included. Moreover, since we will concentrate on two component systems, symmetry energy terms are included as they are also in mean field theories.

II. THE THERMODYNAMIC MODEL

The thermodynamic model has been described in many places [6,7,11]. For completeness and to enumerate the parameters we provide some details.

Assume that the system which breaks up after two ions hit each other can be described as a hot equilibrated nuclear system characterized by a temperature T and a freeze-out volume V within which there are A nucleons ($A = Z + N$). The partition function of the system is given by

$$Q_{Z,N} = \sum \prod_{i,j} \frac{\omega_{i,j}^{n_{i,j}}}{n_{i,j}!} \quad (2.1)$$

Here $n_{i,j}$ is the number of composites with proton number i and neutron number j and $\omega_{i,j}$ is the partition function of a single composite with proton, neutron numbers i, j respectively. The sum is over all partitions of Z, N into clusters and nucleons subject to two constraints: $\sum_{i,j} i n_{i,j} = Z$ and $\sum_{i,j} j n_{i,j} = N$. These constraints would appear to make the computation of $Q_{Z,N}$ prohibitively difficult but a recursion relation exists which allows the computation of $Q_{Z,N}$ quite easy on the computer even for large Z or N [12]. Three equivalent recursion relations exist, any one of which could be used. For example, one such relation is

$$Q_{z,n} = \frac{1}{z} \sum_{i,j} i \omega_{i,j} Q_{z-i, n-j} \quad (2.2)$$

The average number of particles of the species i, j is given by

$$\langle n_{i,j} \rangle = \omega_{i,j} \frac{Q_{Z-i,N-j}}{Q_{Z,N}} \quad (2.3)$$

All nuclear properties are contained in $\omega_{i,j}$. It is given by

$$\omega_{i,j} = \frac{V_f}{h^3} (2\pi(i+j)mT)^{3/2} \times q_{i,j,int} \quad (2.4)$$

Here V_f is the free volume within which the particles move; V_f is related to V through $V_f = V - V_{ex}$ where V_{ex} is the excluded volume due to finite sizes of composites. This is the only interaction between clusters we try to simulate. This restricts the validity of the model to low density (i.e., large V). Further, we take V_{ex} to be fixed, independent of multiplicity. In reality, V_{ex} should depend upon multiplicity [18]. We take it to be constant and equal to $V_0 = A/\rho_0$ where ρ_0 is the normal nuclear density and A is the number of nucleons of the disassembling system. As in previous applications, we restrict the model to freeze-out densities less than $\rho/\rho_0 = 0.5$ that is $V \geq 2V_0$. The factor $q_{i,j,int}$ is the internal partition function of the composite. Define $a = i + j$. Then

$$q_{i,j,int} = \exp [Wa - \sigma a^{2/3} - s \frac{(i-j)^2}{a} + aT^2/\epsilon_0]/T \quad (2.5)$$

Here $W = 15.8$ MeV, $\sigma = 18$ MeV, $s=23.5$ MeV and $\epsilon = 16.0$ MeV. The reader will recognise the volume, surface and symmetry energy of the cluster i, j and the contribution to the internal partition function from excited states in the fermi-gas formulation. For $a(= i + j) \geq 5$ we use this formula. For lower masses we simulate no Coulomb case by setting the binding energy of ${}^3\text{He}$ =binding energy of ${}^3\text{H}$ and binding energy of ${}^4\text{Li}$ =binding energy of ${}^4\text{H}$.

For a given a , what are the limits on i (or $j = a - i$)? This is a non-trivial question. In the results we will show, we have taken limits by calculating the drip lines of protons and neutrons as given by the above binding energy formula. Limiting oneself within the drip lines is a well-defined prescription, but is likely to be an underestimation since resonances show up in particle-particle correlation experiments. On the other hand, for a given a , taking the limits of i from 0 to a is definitely an overestimation.

There is another consideration which restricts the validity of the model. We have assumed (Eq.(2.1)) that the standard correction $n_{i,j}!$ takes care of antisymmetry or symmetry of the particles. In the range $T > 3$ MeV and $\rho/\rho_0 < 0.5$ this is usually true. At low temperatures where one might apprehend the usual correction to fail, it survives because many composites appear, thus there is not enough of any particular species to make (anti)symmetrisation an important issue. At much higher temperature the number of protons and neutrons increase but as is well-known, the $n!$ correction takes the approximate partition function towards the proper one at high temperature. We define $y \equiv Z/(Z + N)$ where Z and N are the total proton and neutron numbers of the disintegrating system and the theory works even at low temperatures if y is in the vicinity of 0.5. But for example, at $T=5.0$ MeV and $y=0$ (neutron matter), this is a terrible model. Now the number of neutrons is large and the temperature is not high and Fermi-Dirac statistics must be enforced. This was studied quantitatively in [19]. In our applications of the thermodynamic model we will confine y to be between 0.3 to 0.7 and $T \geq 3$ MeV. This is indeed not very restrictive since this encompasses the drip lines and so the model, which was devised for intermediate energy heavy-ion collisions, will be applicable. For ${}^{124}\text{Sn}+{}^{124}\text{Sn}$ collisions, a much studied case, the value of y is 0.4.

By equation of state (EOS) we mean $p - V$ diagrams for fixed temperatures. This can be obtained by exploiting the equation $p = T \frac{\partial \ln Q_{Z,N}}{\partial V_f}$. From eqs (2.1) and (2.3), this reduces to $p = \frac{T}{V_f} (\sum \langle n_{i,j} \rangle - 1)$ where -1 within the parenthesis corrects for centre of mass motion. The simplicity of this formula suggests that we just have a non-interacting gas with many species with V being replaced by V_f . But this is deceptive. In fact $\sum \langle n_{i,j} \rangle$ (which is the multiplicity) is not fixed but varies as a function of both temperature T and volume V thus this is not anything as simple as a mixture of non-interacting species. It is indeed interactions which make or break clusters to produce the final equilibrium or statistical distribution of fragments. In this sense interactions are also included.

Since ours is a canonical model, we do not need the chemical potentials μ_p (proton chemical potential) and μ_n but we compute them anyway from the relation $\mu = (\frac{\partial F}{\partial n})_{V,T}$. We know the values of $Q_{Z,N}$, $Q_{Z-1,N}$ and $Q_{Z,N-1}$. Since F is just $-T \ln Q$, we compute μ_p from $\mu_p = -T(\ln Q_{Z,N} - \ln Q_{Z-1,N})$ and μ_n from $-T(\ln Q_{Z,N} - \ln Q_{Z,N-1})$. Indeed, the grand canonical version of the thermodynamic model we are solving has been known for a long time in heavy ion collision physics [2]. There the μ_p and μ_n arise naturally. We have checked that the grand canonical values of μ_p and μ_n are indeed very close to the ones we derive by exploiting the canonical partition functions whose values we know numerically. Throughout this work, whenever we plot μ 's we have obtained the values from a canonical calculation. One might think that since our model has many species there should be many μ 's but in fact all μ 's can be expressed in terms of only μ_p and μ_n . Since our model is based solely on phase space, chemical equilibrium is in fact implied.

III. A MEAN-FIELD MODEL

We want to contrast the model above with mean-field theories. Our mean-field calculation uses the simplest model consistent with nuclear matter binding energy, saturation density, compressibility and symmetry energy for asymmetric matter. The potential energy density is taken to be

$$V(\rho_n, \rho_p) = \frac{A_u}{\rho_0} \rho_n \rho_p + \frac{A_l}{2\rho_0} (\rho_n^2 + \rho_p^2) + \frac{B}{\sigma+1} \frac{\rho^{\sigma+1}}{\rho_0^\sigma} \quad (3.1)$$

Here $\rho_0 = 0.16 \text{ fm}^{-3}$ and ρ_n and ρ_p are neutron and proton densities and $\rho = \rho_n + \rho_p$. The dimensionless constant σ and A_u, A_l, B (all in MeV) are chosen to reproduce nuclear matter binding at 16 MeV per particle, saturation density at 0.16 fm^{-3} , compressibility at 201 MeV and symmetry energy at 23.5 MeV. The energy per particle (including kinetic energy) at $T = 0$ is

$$E/A = A_u \frac{\rho_n \rho_p}{\rho \rho_0} + \frac{A_l}{2\rho \rho_0} (\rho_n^2 + \rho_p^2) + \frac{B}{\sigma+1} \left(\frac{\rho}{\rho_0}\right)^\sigma + 22.135 \times \left[\frac{\rho_p}{\rho} \left(\frac{2\rho_p}{\rho_0}\right)^{2/3} + \frac{\rho_n}{\rho} \left(\frac{2\rho_n}{\rho_0}\right)^{2/3} \right] \quad (3.2)$$

The values of the constants are: $\sigma = 7/6$; $A_u = -379.2 \text{ MeV}$; $A_l = -334.4 \text{ MeV}$; $B = 303.9 \text{ MeV}$.

The Hartree-Fock energy of an orbital is given by

$$\epsilon = p^2/2m + A_u(\rho_u/\rho_0) + A_l(\rho_l/\rho_0) + B(\rho/\rho_0)^\sigma \quad (3.3)$$

The value of μ_p is found by solving for a given ρ_p and $\beta = 1/T$

$$\rho_p = \frac{8\pi}{h^3} \int_0^\infty \frac{p^2 dp}{\exp(\beta(\epsilon_p - \mu_p)) + 1} \quad (3.4)$$

Similarly μ_n is extracted from ρ_n . The pressure has contributions from kinetic energy and the potential energy. The contribution from the kinetic energy is calculated from well-known Fermi-gas model formula. Contribution to pressure from interaction is

$$p_{skyrme} = \frac{A_u}{\rho_0} \rho_n \rho_p + \frac{A_l}{2\rho_0} [(\rho_n)^2 + (\rho_p)^2] + \frac{\sigma}{\sigma+1} B \left(\frac{\rho}{\rho_0}\right)^\sigma \rho \quad (3.5)$$

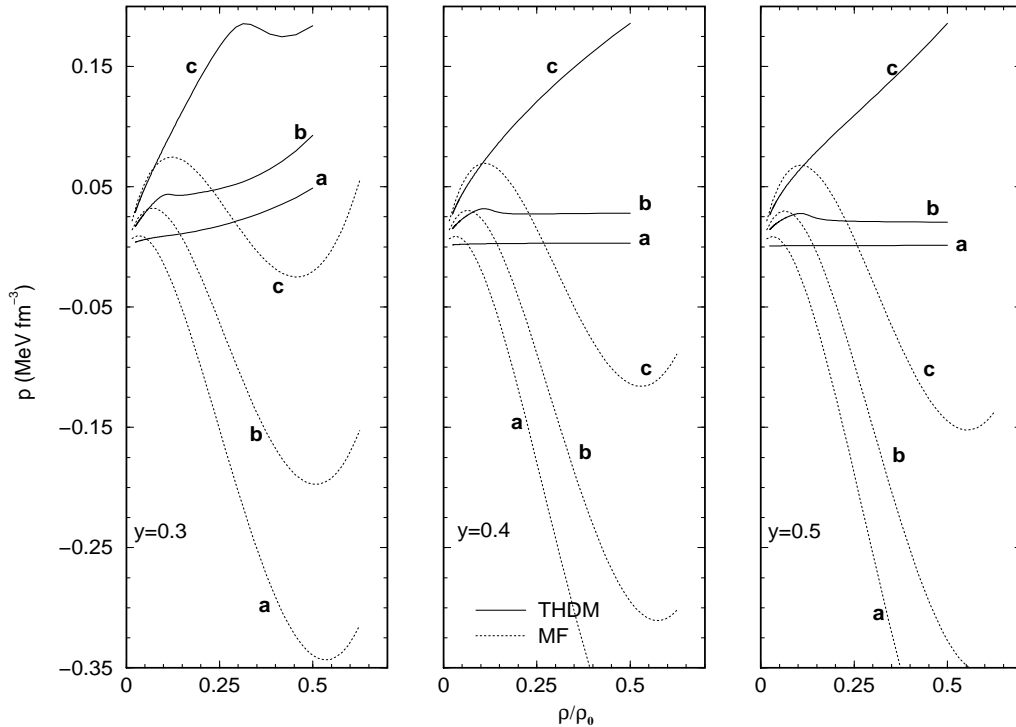


Fig.1: The EOS in the two models at different temperatures [(a) 4 MeV, (b) 7 MeV and (c) 10 MeV] for y 0.3, 0.4 and 0.5.

IV. EOS IN THE TWO MODELS

Fig. 1 compares the $p - V$ diagrams at constant temperature for the two models. We restrict the value of $y = \rho_p / (\rho_p + \rho_n)$ between 0.3 and 0.5 and ρ / ρ_0 between 0 and 0.5 because outside these ranges the validity of the thermodynamic model is significantly reduced although the mean-field model has no obvious limitations. The striking feature of Fig. 1 is the huge difference in the EOS of the two models. The mean-field model is characterised by large regions of spinodal instability, regions where $\frac{\partial p}{\partial \rho}$ is negative. In exact theories, $\frac{\partial p}{\partial \rho}$ will not be negative. In the scale of mean-field theories, such negative slopes are almost absent in the thermodynamic model (they are present when plotted in an expanded scale, see Fig. 3) and one would be tempted to conclude that the thermodynamic model is a better representation for the behavior of a real system.

V. ISOSPIN FRACTIONATION

Isospin fractionation is a well-established experimental phenomenon [20]. If the disintegrating system has a given $N/Z > 1$ then, after collision, the measured n_n/n_p ratio (where n_n, n_p are measured single neutron and proton yields respectively) is higher than N/Z . Similarly, the ratio of measured $\langle n_{1,2} \rangle / \langle n_{2,1} \rangle$ is higher than what one might expect from the N/Z ratio of the disintegrating system. This then implies that if there is a large chunk left after the breakup it must have a n/z ratio lower than original N/Z since the total number of neutrons and protons must be conserved. If we characterise n/z ratio etc. in terms of the parameter y we have been using, then if y_{source} is less than 0.5, then y of the large chunk is greater than y_{source} and $\langle n_p \rangle / (\langle n_p \rangle + \langle n_n \rangle)$ is less than y_{source} .

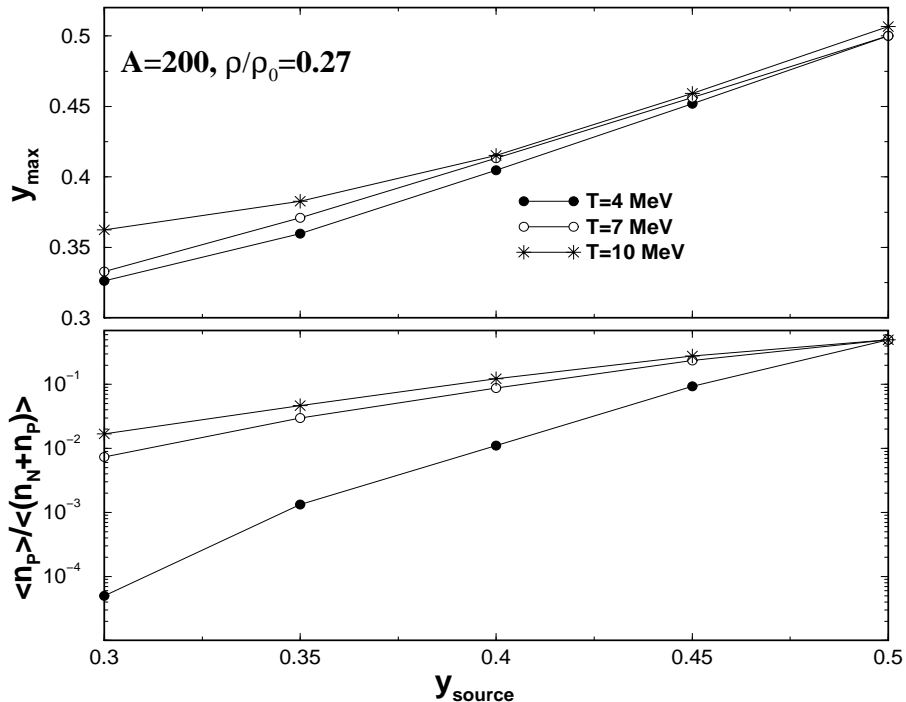


Fig.2: Example of isospin fractionation in the thermodynamic model. y of the largest cluster (top panel) is plotted in the top panel. This y is larger than the y value of the whole system. The lower part of the figure shows that the gas of nucleons is very rich. For example for $y=0.4$ and $T=7-10$ MeV, $\langle n_n \rangle \approx 10\langle n_p \rangle$ while for $T=4$ MeV, $\langle n_n \rangle \approx 100\langle n_p \rangle$.

A priori, it would seem difficult to get this aspect out of a mean-field model but in a seminal piece of work Muller and Serot have demonstrated how this might come about [21,22]. In mean-field theory, analogous to mechanical instability ($\frac{\partial p}{\partial \rho} < 0$) there appears regions of chemical instability, i.e., $\frac{\partial \mu_p}{\partial y} < 0$ (or $\frac{\partial \mu_n}{\partial y} > 0$) when two kinds of particles are involved. One can avoid this unphysical region of chemical instability but then needs to consider splitting the system into two parts, each homogeneous but distinct from each other, one belonging to the liquid phase with higher y value and the other to the gas phase with lower y value. One consequence of this is that the phase transition takes place

neither at constant pressure nor at constant volume and what would have been a first order phase transition, becomes a second order phase transition.

In the thermodynamic model, isospin fractionation happens naturally. In general, the model has, as final products, all allowed composites, a, b, c, d, \dots where the composite labelled a has $y_a = i_a / (i_a + j_a)$ where i_a, j_a is the number of protons and number of neutrons respectively in the composite a . The only law of conservation is $Z = \sum_a i_a \times n_a$ and $N = \sum_a j_a \times n_a$. So a large chunk can exist with higher y than that of the whole system and populations of other species can adjust to obey overall conservation laws. Whatever partition lowers the free energy will happen. The thermodynamic model is dramatically different from mean field models. The most significant difference is that in the thermodynamic model, if we prescribe that dissociation takes place at $\rho/\rho_0=0.3$ we still have only clusters with normal nuclear density and properties and also nucleons. It is just that there are empty spaces between different clusters and nucleons in the region of dissociation. But in mean field models $\rho/\rho_0=0.3$ will imply that the nuclear matter is uniformly stretched to this density. While this can happen as a transient phenomenon such as in transport calculation, whether this can also exist as an equilibrium situation is highly questionable.

An example of isospin fractionation in the thermodynamic model is shown in Fig. 2. The formalism developed in section II can also be extended to calculate the average number of nucleons and protons (or neutrons) in the largest cluster. For brevity we do not write down the formulae here but these are straightforward extensions of Eqs.(2.7) and (2.8) given in [6]. Fig. 2 shows results from such a calculation. If y of the disintegrating system is less than 0.5, the y value of the largest cluster is larger than that of the source. Correspondingly, $(\langle n_p \rangle) / (\langle n_p \rangle + \langle n_n \rangle)$ is much smaller than y_{source} . [It should be mentioned that the number of protons and neutrons will be augmented from decays of hot composites, so what is plotted in Fig. 2 is not what will actually be observed in experiments]. Further the isospin fractionation happens whether the dissociation takes place at constant volume or constant pressure.

In this and many other aspects, the thermodynamic model is very similar to the Lattice Gas Model (LGM) with isospin dependence. For an accurate solution of LGM one has to give up the mean-field approach and obtain results by Monte-Carlo simulation. Here also many composites are produced with many different y values [23,24]. Isospin fractionation happens naturally [24].

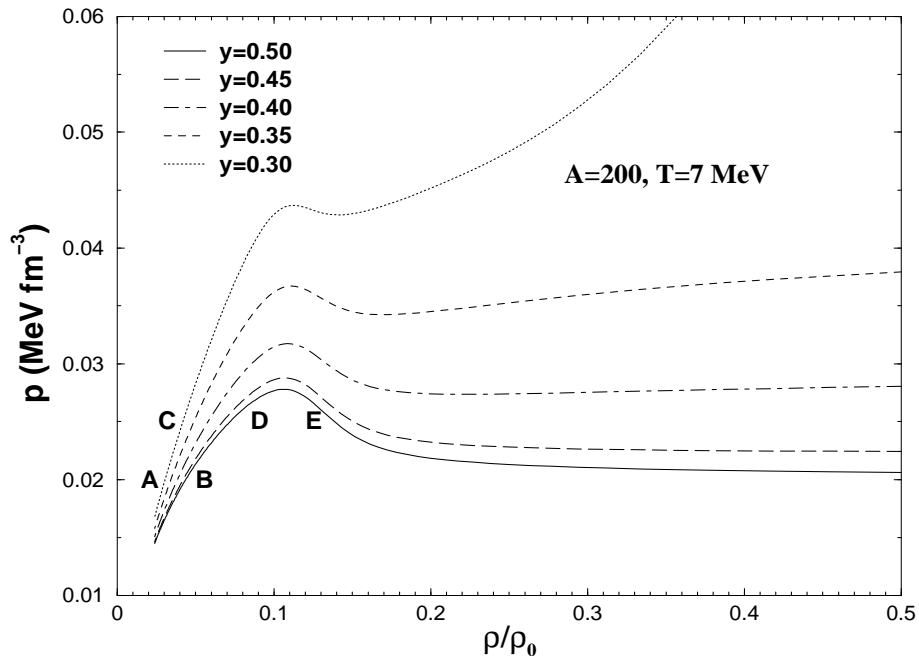


Fig.3: EOS ($p - \rho$) in the thermodynamic model at $T=7.0$ MeV but for different y 's.

VI. INSTABILITY IN THE THERMODYNAMIC MODEL

Fig. 1 shows that compared to the mean-field model, regions of mechanical instability with $\frac{\partial p}{\partial \rho} < 0$ nearly disappear in the thermodynamic model. In an expanded scale, they are more readily seen (Fig. 3) where we have drawn $p - \rho$ diagram for a constant temperature $T=7.0$ MeV but different y 's.

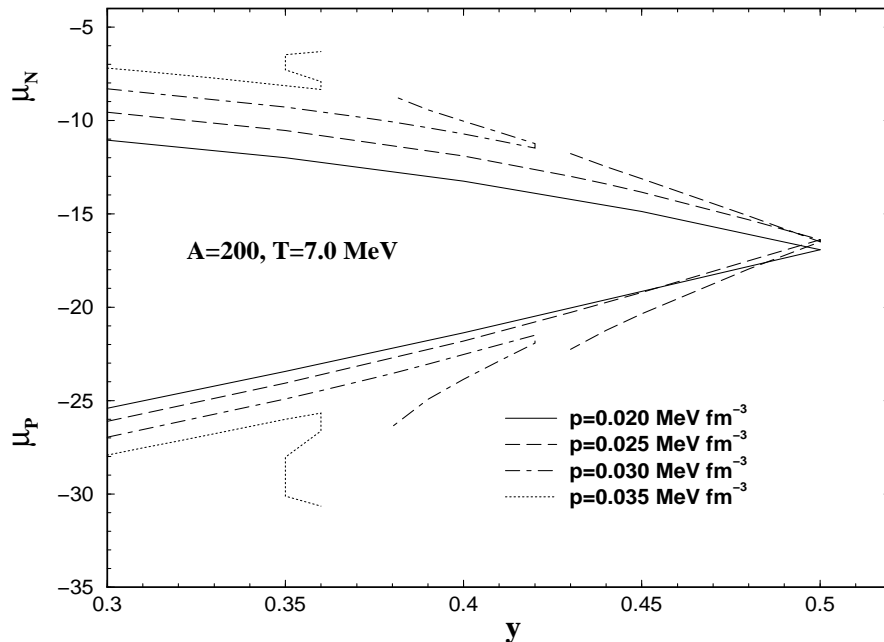


Fig.4: μ_P and μ_N as a function of y . Here $T=7$ MeV.

We clearly have some regions of mechanical instability. Chemical instability implies $(\frac{\partial \mu_p}{\partial y})_{p,T} < 0$. We investigate that now. At $T=7$ MeV, we have drawn μ_p (and μ_n) at four pressures (Fig. 4). To get an understanding of the behaviour, we need to also look at Fig. 3. At the lowest pressure shown, $p = 0.02$ MeV fm^{-3} (Fig. 4), the horizontal constant pressure curve cuts the isothermals (Fig. 3) at the low density side only (between A and B) and μ_p rises monotonically between $y = 0.3$ and $y = 0.5$. The next constant pressure curve, at $p = 0.025$ MeV fm^{-3} (Fig. 4) cuts all isothermals (Fig. 3) at low density side ($\rho/\rho_0 < 0.1$) between C and D and a few isothermals at higher density side. Between C and D , y increases as does μ_p . The points marked D and E have the same values of p and T but very slightly differing values of μ_p . As we move to the right from E along the line $p=0.025$ MeV fm^{-3} the value of y drops as also the value of μ_p . We forego describing graphs at other pressures but the figure shows there is a very small region where $\frac{\partial \mu_p}{\partial \rho}$ is negative (Fig. 4, $p = 0.035$ MeV fm^{-3}). The not so obvious feature is the appearance of two branches in both μ_p and μ_n (i.e., for example, the $p = 0.025$ MeV fm^{-3} curve). The two branches would merge for a Van der Waals fluid and thus the appearance of two branches indicates departure from a Van der Waals fluid.

VII. COMPARISON WITH VAN DER WAALS FLUID

For a Van der Waals fluid with Maxwell construction, the following behaviour will be seen [25] as we move along an isothermal in a $\mu - \rho$ plane, provided we are below the critical temperature. If we start with very small density we are in the gas phase. As the density rises, the chemical potential changes till it reaches the coexistence region. In this region $\mu_{gas} = \mu_{liq}$ and as the density changes the chemical potential remains unchanged but more particles change from the gas phase to the liquid phase. This remains the situation till a high density is reached when all the particles are in the liquid phase.

The situation in the thermodynamic model is depicted in Fig. 5. The model is inapplicable to high density situation, so we cut-off ρ at $\rho/\rho_0 = 0.5$. We have two chemical potentials μ_p and μ_n and to compare to a Van der Waals fluid, we consider the combination $\mu = y\mu_p + (1 - y)\mu_n$ (for $y=0.5$, $\mu_p = \mu_n$ any way). At $T=7.0$ MeV we show in the left panel of Fig.5 the behaviour of μ at $y = 0.5, 0.4$ and 0.3 . For the $y=0.5$ curve we also depict schematically what the behaviour would have been if we had a Maxwell-corrected Van der Waals fluid. From some point *A*, the chemical potential would remain unchanged (shown by a horizontal line ending at *B* which is the end-point of our density). A more familiar plot is μ against pressure p for a fixed temperature. This is shown in the right panel for our model. For a Van der Waals fluid, the segment from *A* to *B* would simply collapse to the point *A*.

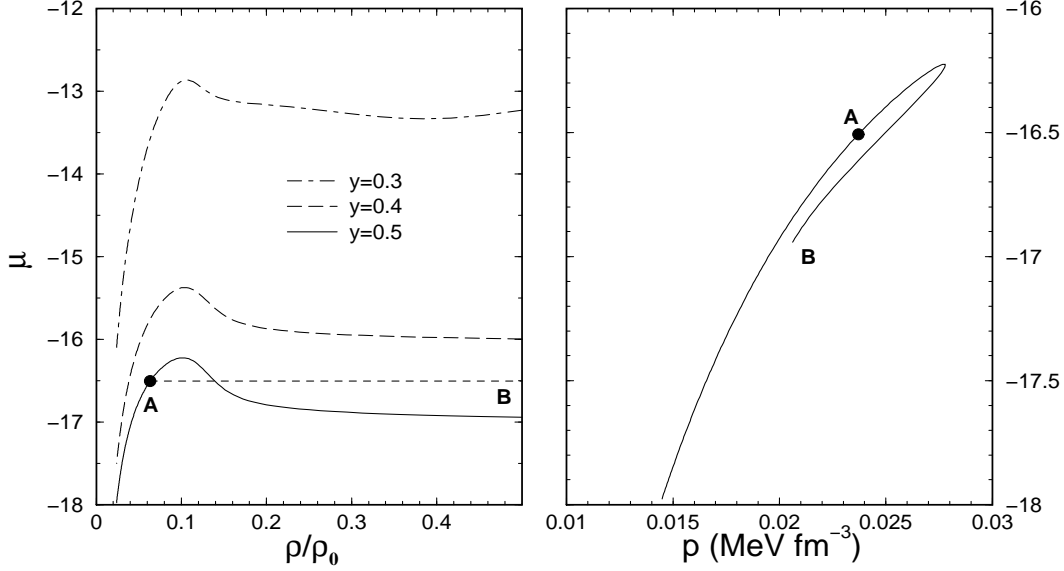


Fig.5: $\mu = y\mu_p + (1 - y)\mu_n$ as a function of ρ/ρ_0 for different y 's(left panel). The temperature is 7 MeV. In the right panel the behaviour of μ is shown as a function of pressure p for $y = 0.5$ and $T = 7$ MeV.

VIII. SPECIFIC HEATS IN THE MODEL

In [6] where the thermodynamic model was first studied for phase transitions, it was pointed out that for a given density ρ , the specific heat per particle C_V/A tends to ∞ at a particular temperature when the particle number A tends to ∞ . Since $C_V = (\frac{\partial E}{\partial T})_V = T(\frac{\partial S}{\partial T})_V = -T(\frac{\partial^2 F}{\partial T^2})_V$, a singularity in C_V signifies a break in the first derivative of F , the free energy and a first order phase transition. The model in [6] considered one kind of particle although binding energy, surface energy etc. were chosen to mimic the nuclear case. We see similar effect here when we take into account two kinds of particles explicitly (Fig. 6, see also [7]). The calculated C_V/A becomes progressively sharply peaked as A increases for all y values between 0.3 and 0.5. This behaviour of the specific heat is very different from that of mean field model of nuclear matter where the specific heat at constant volume varies smoothly from a low temperature Fermi gas to an ideal gas as T increases. In a thermodynamic model with fragmentation, this behaviour is modified by the surface energies that arise in the multifragmentation of the original nucleus into clusters of different sizes. The peak in the specific heat occurs at the point where the largest cluster suddenly disappears. This behaviour is nuclear boiling.

Specific heat per particle C_p/A in the model has not been considered before. A rigorous discussion would first need a proper prescription for eliminating the unphysical region $\frac{\partial p}{\partial \rho} < 0$ (even though these regions are much less visible than in mean field model) by a Maxwell like construction. The reason for this remark is the following. One could try utilising the relation $C_p = C_V - \frac{T(\partial p/\partial T)_V^2}{(\partial p/\partial V)_T}$. However there are regions where $(\partial p/\partial V)_T$ is positive (mechanical

instability) so that C_p can turn out to be less than C_V . Alternately we can try to deduce C_p directly from EOS. Consider again Fig. 3 and first let us limit to $y=0.5$ curve (all the curves are at $T=7.0$ MeV). Points D and E have the same pressure and temperature but different energy contents thus C_p at $T=7.0$ MeV and $p=0.025$ MeV fm^{-3} is ∞ . (The difficulty in this sort of argument is that points D and E are not contiguous points thus dE is not a differential.) But this is not the only p value where $C_p = \infty$. Using similar argument: for $y=0.5$ and $T=7.0$ MeV C_p is ∞ at pressure between 0.021 MeV fm^{-3} and 0.027 MeV fm^{-3} . With a Maxwell like construction this range of p values should converge to a single p value but at this p the value of C_p will go to ∞ . As another example, looking now at $y=0.35$ curve, at $T=7.0$ MeV, C_p becomes ∞ in the pressure range 0.034 - 0.036 MeV fm^{-3} .

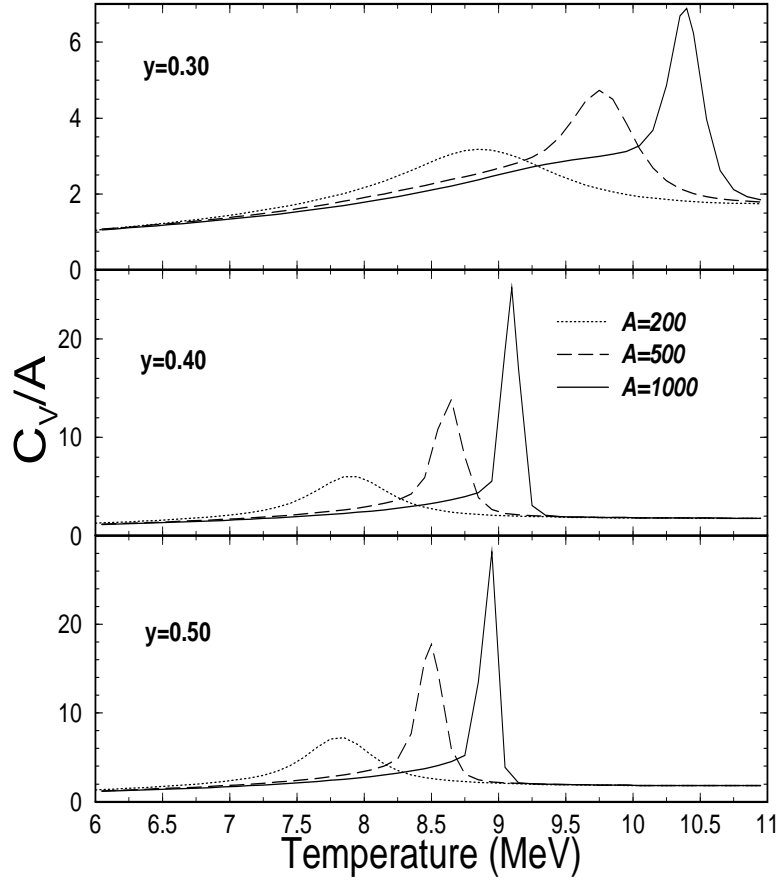


Fig.6: C_V/A as a function of temperature for systems of 200, 500 and 1000 particles with different proton fractions.

IX. SUMMARY

We looked at several features of a thermodynamic model (which has seen many applications in data fitting) and a mean field model. The equations of state generated by the two models are very different. Specifically, the thermodynamic model has an EOS which becomes very flat with density and volume and this behaviour resembles a real system undergoing a first order phase transition. By contrast (see Fig.1) a mean field theory model has large regions of spinodal instability. When the system enters the region of instability, it fragments into pieces. This fragmentation is directly included in the thermodynamic model and this is the reason for relative flatness in the EOS. The cluster distribution readjusts itself with changes in V or ρ to maintain a nearly constant pressure. Isospin fractionation seen in experiments can be also obtained in the mean field model but it requires a bifurcation in the isotopic space. It also requires that during dissociation neither pressure nor volume remain constant. By contrast, isospin fractionation occurs naturally in the thermodynamic model and can happen either at constant volume or at constant pressure. Large differences between these two models also appear in the calculation of C_V . The thermodynamic model has a strong peak in C_V whose origin are surface energy terms in the multifragmentation process which is lacking in a mean

field model of homogeneous nuclear matter. This peak is associated with the phenomenon of nuclear boiling and the sudden disappearance of the largest cluster.

X. ACKNOWLEDGMENT

This work is supported in part by the Natural Sciences and Engineering Research Council of Canada and the U.S. Department of Energy Grant No. DE FG02-96ER40987.

- [1] A. Z. Mekjian, Phys. Rev. Lett. **38**, 640 (1977)
- [2] S. Das Gupta and A. Z. Mekjian, Phys. Rep. **72**, 131 (1981)
- [3] J. P. Bondorf, A. S. Botvina, A. S. Iljinov, I. N. Mishustin, and K. Sneppen, Phys. Rep. **257**, 133 (1995)
- [4] J. Randrup and S. E. Koonin, Nucl. Phys. **A471**, 355c (1987)
- [5] D. H. E. Gross, Phys. Rep. **279**, 119, (1997)
- [6] S. Das Gupta and A. Z. Mekjian, Phys. Rev **C57**, 1361 (1998)
- [7] P. Bhattacharyya, S. Das Gupta and A. Z. Mekjian, Phys. Rev **C60**, 054616 (1999)
- [8] P. Bhattacharyya, S. Das Gupta and A. Z. Mekjian, Phys. Rev **C60**, 064625 (1999)
- [9] S. Pratt and S. Das Gupta, Phys. Rev. **C62**, 044603 (2000)
- [10] A. Majumder and S. Das Gupta, Phys. Rev. **C61**, 034603 (2000)
- [11] S. Das Gupta, A. Z. Mekjian and M. B. Tsang, Advances in Nuclear Physics, vol.26, 91 (2001)
- [12] K. C. Chase and A. Z. Mekjian, Phys. Rev **C50**, 2078 (1994)
- [13] M. B. Tsang et al., Phys. Rev. **C64**, 054615 (2001)
- [14] S. J. Lee and A. Z. Mekjian, Phys. Rev. **C63**, 044605 (2001)
- [15] K. A. Bugaev, M. I. Gorenstein, I. N. Mishustin and W. Greiner, Phys. Rev **C62**, 044320 (2000)
- [16] K. A. Bugaev, M. I. Gorenstein, I. N. Mishustin and W. Greiner, Phys. Lett. **B498**, 144 (2001)
- [17] J. B. Elliott and A. S. Hirsch, Phys. Rev. **C61**, 054605 (2001)
- [18] A. Majumder and S. Das Gupta, Phys. Rev. **C59**, 845 (1999)
- [19] B. K. Jennings and S. Das Gupta, Phys. Rev. **C62**, 014901 (2000)
- [20] H. S. Xu et al., Phys. Rev. Lett. **85**, 716 (2000).
- [21] H. Muller and B. D. Serot, Phys. Rev **C52**, 2072 (1995)
- [22] H. Muller and B. D. serot, *Isospin Physics in Heavy-Ion Collisions at Intermediate Energy*, edited by B.A. Li and W. U. Schroder (Nova Science Publishers, Inc.,Huntington, New York, 2001)
- [23] J. Pan and S. Das Gupta, Phys. Rev. **C57**, 1839 (1998)
- [24] Ph. Chomaz and F. Gulminelli, Phys. Lett **B447**, 221 (1999).
- [25] F. Reif, *Fundamentals of statistical and thermal physics* (McGraw-Hill, New York, 1965), ch.8.